Lasers in Manufacturing Conference 2023

# Laser mediated fusing of paper materials

Florian Lull[a,*], Dr. Martin Zahel[b], Dr. Michael Panzner[a], Tom Schilling[b]

[a]*Fraunhofer Institute for Material and Beam Technology, Winterbergstraße 28, 01277 Dresden, Germany*
[b]*Papiertechnische Stiftung, Pirnaer Straße 37, 01809 Heidenau, Germany*

**Abstract**

This paper presents the results of fundamental studies on the interaction of laser radiation with classical paper materials regarding the melting of the main paper components cellulose, hemicellulose and lignin. Different papers were irradiated with the laser radiation of a carbon monoxide (CO) laser. Fluence-dependent interaction regimes, the dynamics of the flash pyrolysis and chemical changes due to irradiation are discussed. Using a high-speed camera, a liquid intermediate state could be observed as a result of the irradiation. This is decomposed into gaseous reaction products by a highly dynamic boiling process. In addition to the time resolved investigations, extensive FTIR studies were performed.

Keywords: CO laser; paper; pulp; melting

## 1. Introduction

Cellulose is the most abundant organic polymer on earth [O'Sullivan, 1997] and, as the main component of paper and paper products, it is impossible to imagine daily life without it. In addition to the paper industry, important areas of application include the clothing industry (e. g. cotton), the building materials industry (as a flow improver) and, above all, the packaging industry in the form of paper itself or cellophane film.

In addition to various form-fit joining processes, joints in the packaging industry are mainly made by adhesive bonding. In view of growing environmental awareness, the importance of good recyclability of packaging is constantly increasing. Many established adhesives cause deposits on machine parts as well as dirt specks in papers and lead to machine downtimes and increased scrap formation [Delagoutte, 2015; Hamann, 2015]. Separation of larger particles is technologically possible to about 70 - 95 %. However, smaller adhesive residues often have to be passivated and fixed in the pulp by the increased use of process chemicals. This is usually only incompletely successful. Joining paper materials by melting and welding without additional material would be an excellent alternative.

Next to the industrial motivation is the scientific one. A liquid phase is prevented due to the lack of a suitable temperature range between melting and pyrolytic decomposition. The first studies on melting of cellulose

were carried out in the 70's by Back and Nordin [Nordin et al, 1974; Back et al, 1974; Back et al, 1973]. Back predicted melting by rapid heating to 450 °C using a pulsed CO2 laser followed by cooling in tenths of milliseconds by liquid nitrogen. A decrease in the fibrous structure, the formation of bubble-like structures, and an increase in the amorphous phase were observed. The resulting reaction products were studied by Suzuki et al [Suzuki et al, 1983], among others, and identified as monosaccharides and oligosaccharides due to chain scission and other transformation reactions. A liquid intermediate state during the decomposition of cellulose was already described in the Broido-Shafizadeh model in the late 1970s [Shafizadeh et al, 1979]. A visual observation of the so-called active cellulose was successful due to its short lifetime with a high-speed camera [Boutin et al, 1998; Boutin et al, 2002].

During irradiation the investigations with pulsed CO laser radiation were examined using a high-speed camera and after irradiation microscopically and IR spectroscopically. When the papers are melted or decomposed, different IR spectra are formed, which were used for differentiation. The hydrogen bonding network between the individual polymer chains of naturally occurring cellulose is referred to as the cellulose I configuration [O'Sullivan, 1997]. In the case of melting, these hydrogen bonds are broken and the molecular strands are free to move. When resolidifying, a different bonding network is formed, also called cellulose II configuration. This is thermodynamically more stable and thus energetically more sensible. In contrast to pyrolytic decomposition, complete cellulose polymers with modified intermolecular bonds are present after melting and resolidification. In pyrolysis, on the other hand, the chain length is reduced by chain scission.

## 2. Material and methods

### *2.1. Material and methods*

Four different paper substrates with different compositions were investigated. Table 1 lists the main components and some pulp properties. The percentage of carbonyl groups influences the aging of the paper [Bansa et al, 1979]. Lignin indicates the percentage of lignin in the paper. S5 and S18 indicate the solubility in 5 % and 18 % sodium hydroxide solution, respectively. S5 thus describes the amount of low molecular weight compounds from 5-fold sugars contained, while S18 describes the amount of all hemicelluloses. Ashes represent all inorganic compounds in the paper. CI is the crystallinity index according to Segal [Segal et al, 1959].

Table 1. Components and pulp properties of the investigated paper substrates.

| Paper | Linters | Sulfate | Sulfite | CTMP |
|---|---|---|---|---|
| Carbonyl groups / % | 2 | 2 | 7 | 1 |
| Lignin / % | 0.34 | 0.16 | 0.19 | 30.21 |
| S5 / % | 1.72 | 8.54 | 11.95 | 5.18 |
| S18 / % | 1.44 | 14.82 | 11.49 | 4.87 |
| Ashes / % | 0.15 | 0.23 | 0.30 | 0.66 |
| CI / % | 0.87 | 0.82 | 0.80 | 0.75 |

### *2.2. Characterization*

Both visual appearance and morphology were examined by light microscopy (VHX 5000, Keyence). Threshold fluences were determined using the method of Liu [Liu, 1982].

All spectra were recorded by FTIR-ATR spectroscopy (Tensor 27, Bruker). The differentiation between the native cellulose I configuration and the thermodynamically more stable cellulose II configuration is made in the fingerprint region of the spectrum, between 850 $cm^{-1}$ and 1450 $cm^{-1}$ [Nelson et al, 1964]. During the transition from cellulose I to II, sharply defined individual peaks are combined into broader ones as well as shifted to lower wave numbers. The total crystallinity index is used to determine the ratio of the amorphous to the crystalline subregions. This is still valid for the transition from cellulose I to II [Nelson et al, 1964; Hurtubise et al, 1960].

The dynamic of the flash pyrolysis were studied with a high-speed camera (Fastcam SA-X2, Photron Limited) and recorded with 12,500 frames per second. The high-speed recordings allow a general description of the flash pyrolysis as well as the classification into four characteristic time ranges according to objective visual features.

### *2.3. Laser system*

The irradiation experiments were performed with a pulsed carbon monoxide (CO) laser (TruFlow 1500 (CO), Trumpf). Its photon energy at a wavelength of 5.6 µm is close to the binding energy of the structure-giving hydrogen bonds. Due to the high pulse energies, the irradiation was performed defocused by about 100 mm. This ensures sufficiently low fluences and a suitable ablation diameter for the investigations. The focal diameter was approx. 244 µm, the maximum average power 1600 W and the pulse duration approx. 30 ms.

## 3. Results and discussion

### *3.1. Threshold fluence and fluence regimes*

When paper is irradiated with CO laser radiation, a color change (browning) of the fibers occurs above a material-specific threshold fluence without material removal (Fig. 1 a) and b)). This indicates the beginning of a chemical decomposition in the form of hydrolysis or cleavage of hydroxyl groups [Shimazu et al, 1966]. A partial chemical transition takes place, mainly in the amorphous subregions of the cellulose [Kolar et al, 2000]. With further increase of the laser fluence a second threshold fluence is reached, above which ablation and pyrolytic decomposition of fibers takes place (Fig. 1 c) and d)). After irradiation, solidified bubble-like residues with a diameter of 10 to 100 µm can be observed in the ablation area. These indicate the presence of an intermediate liquid phase as well as the coexistence with a gaseous phase.

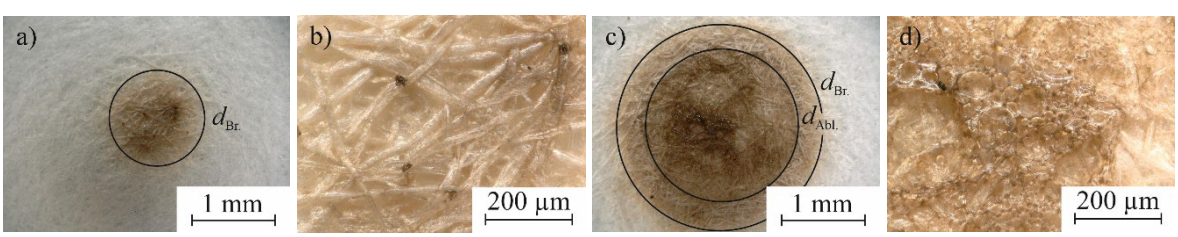


Fig. 1. Sulfate pulp after irradiation with a peak fluence of 0.74 $Jcm^{-2}$ (a) and b)) and of 2.08 $Jcm^{-2}$ (c) and d)).

In the case of sulfate and sulfite pulp, the bubbles occur more frequently, which can be explained by the high content of hemicellulose and inorganic additives (Fig. 2). Hemicellulose is already decomposed into mono- and oligosaccharides at temperatures of 230 °C to 330°C [Shimazu et al, 1966; Yeo et al, 2019; Yang et al, 2007]. The CTMP substrate shows no blistering, but accumulations of carbon-rich compounds. These are a consequence of the high lignin content, which has the highest weight percentage of carbonaceous residues after decomposition compared to the other main paper components [Yang et al, 2007].

A comparison with the paper properties shows a negative correlation of the threshold fluences with the proportions of hemicellulose, lignin and inorganic additives. This indicates that a large part of the radiation is not absorbed by the cellulose but by other paper constituents and then transferred to the cellulose fibers in the form of heat. A positive correlation exists between threshold fluences and crystallinity index. A low crystallinity index corresponds to a high volume fraction of amorphous cellulose. In this regions, chemical transformation processes preferentially take place [Kolar et al, 2000], resulting in increased removal.

Table 2. Threshold fluences of the browning and the ablation regime.

| Paper | $H_{thr.,Br.}$ / Jcm$^{-2}$ | $H_{thr.,Abl.}$ / Jcm$^{-2}$ |
|---|---|---|
| Linters | 0.62 ± 0.10 | 1.03 ± 0.11 |
| Sulfate | 0.50 ± 0.05 | 0.85 ± 0.04 |
| Sulfite | 0.40 ± 0.03 | 0.69 ± 0.12 |
| CTMP | 0.38 ± 0.02 | 0.47 ± 0.02 |

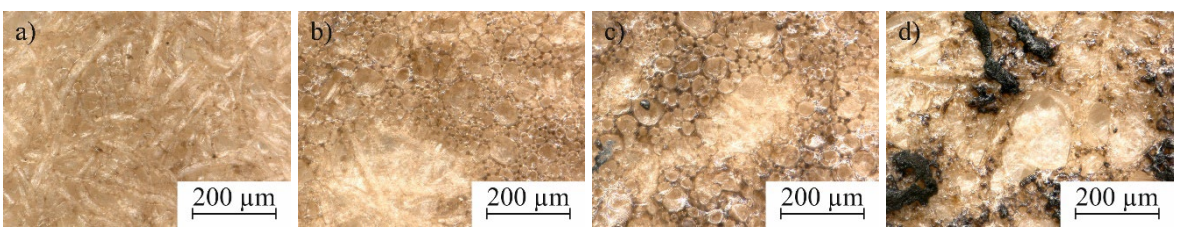


Fig. 2. Substrates after irradiation with a peak fluence of 1.02 Jcm$^{-2}$. a) linters, b) sulfate, c) sulfite, d) CTMP.

### *3.2. Short time melting and flash pyrolysis*

As a result of the irradiation, a highly dynamic, pyrolytic decomposition of the paper takes place. This can be divided into four time ranges by means of high-speed videography according to objective, visual aspects.

Time range 1: In the first milliseconds after the start of the irradiation (Fig. 3 “0.00 ms”), there is a slight movement of the fibers propagating from the center of the irradiation. This is the only observable change during irradiation with fluences in the browning regime ($H_{thr.,Br.} < H < H_{thr.,Abl.}$). The beginning decomposition of the cellulose in the amorphous subregions as well as the release of internal stresses is visible. With increasing fluence, a decrease of the first time range can be observed. The laser radiation rises to the intensity required for decomposition only after a certain time. At higher pulse energies, this rising edge of the pulse is steeper and the decomposition intensity is reached more quickly.

Time range 2: For fluences above the ablation threshold, the second phase begins after a few milliseconds. Due to the high fluences, the formation of a melt-like state starts in the center of the irradiation and spreads outward (Fig. 3 “9.12 ms“ and “12.00 ms“) until a constant diameter is reached (Fig. 3 “24.80 ms“). The simultaneous presence of liquid and gaseous reaction products and the sudden expansion of the latter leads

to highly dynamic boiling during the irradiation, also know as reactive boiling. The extraction of matter occurs by conversion to the liquid state and subsequently to volatile gaseous products [Shafizadeh et al, 1979]. For the duration of the laser pulse, a constant energy input and thus conversion and ablation takes place.

Time range 3: At the end of the irradiation (Fig. 3 “29.36ms”), the third time range of the decomposition begins, which is referred to below as the primary life time (of the liquid substance after a single energy input). Without further energy input, the conversion to gaseous products decreases and the decomposition of the gas-liquid mixture begins (Fig. 3 “38.72 ms“). During this process, smaller bubbles combine to form larger ones, which collapse above a critical size. With increasing fluence, a decrease in primary life time can also be quantified. This is due to the increased amount of energy introduced. At higher fluences and thus more energy in the system after irradiation, matter can be transferred quickly from the liquid in the gaseous phase.

Time range 4: After the decay of the larger bubbles, the fourth time range begins, which will be referred to below as the secondary life time (of the liquid substance after a single energy input). In this phase, decomposition is largely complete. The movement observed in the irradiated area can be attributed to solidification processes of the liquid decomposition products (Fig. 3 “53.28 ms“). The secondary life time shows an increase with increasing fluence, which can also be attributed to the increased amount of energy in the material. At higher fluences, more residual heat remains in the material after boiling. More time is needed to complete the final conversion reactions and to distribute the heat.

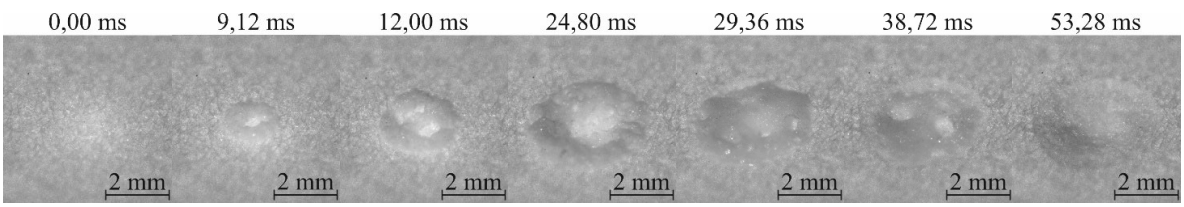


Fig. 3. Flash pyrolysis of a linters substrate due to irradiation at a peak fluence of 2.20 Jcm$^{-2}$ ($H > H_{thr.Abl.}$).

### *3.3. IR spectroscopy*

The IR spectra of the samples after irradiation (Fig. 4 left) show a decrease in peak intensities with increasing fluence, in particular between 1030 cm$^{-1}$ and 1161 cm$^{-1}$ (dashed lines). Especially, the decrease is visible from a fluence of 2.1 Jcm$^{-2}$. This is due to the ablation threshold fluence of 1.03 Jcm$^{-2}$ (linters) being exceeded. After extraction of all water-soluble pyrolysis products (Fig. 4 right), the peaks reappear. The substances that changed the spectrum are thus water-soluble and therefore not molten cellulose. The remaining low intensity of the band at 1109 cm$^{-1}$ is due to non-water soluble reaction products.

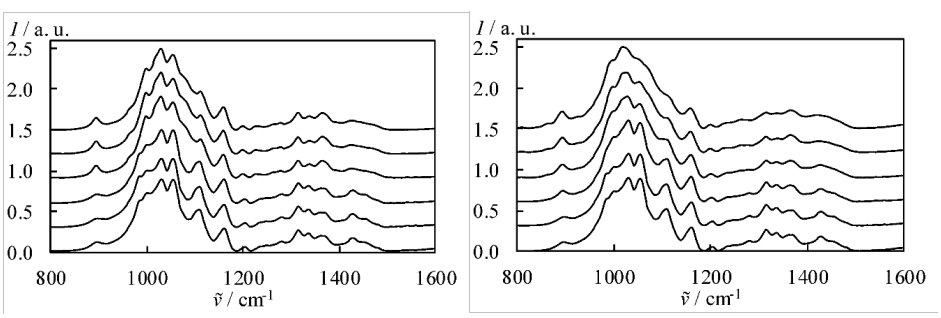

Fig. 4. IR spectra of an irradiated (left) as well as irradiated and aqueous extracted (right) linters substrate in dependence of the laser fluence. Bottom to top: 0.0 $Jcm^{-2}$, 0.3 $Jcm^{-2}$, 0.5 $Jcm^{-2}$, 2.1 $Jcm^{-2}$, 5.2 $Jcm^{-2}$, 13.7 $Jcm^{-2}$.

The crystallinity index of the samples before extraction shows a decrease with increasing fluence below the ablation threshold (Fig. 5 left). This decrease is due to chemical transformation reactions responsible for the color change. Above the threshold fluence, the trend flattens out and the crystallinity index remains more or less unchanged. A strong decrease correlates with the content of hemicellulose and inorganic additives (sulfate and sulfite) or lignin (CTMP).

After aqueous extraction (Fig. 5 right), the crystallinity index at low fluences ($H < H_{thr.,Abl.}$) shows fluctuations around the values without extraction, indicating that few water-soluble products are formed in this fluence range. Above the threshold fluence, stagnation is again observed. Nevertheless, the crystallinity index is generally higher than the values of the unirradiated substrates, which can be interpreted as an increase in the crystalline material content. The sulfate, sulfite and CTMP pulps exhibit a higher crystallinity index after aqueous extraction even without irradiation. Thus, it can be assumed that the material contains water-soluble compounds from the beginning, which lower the crystallinity index.

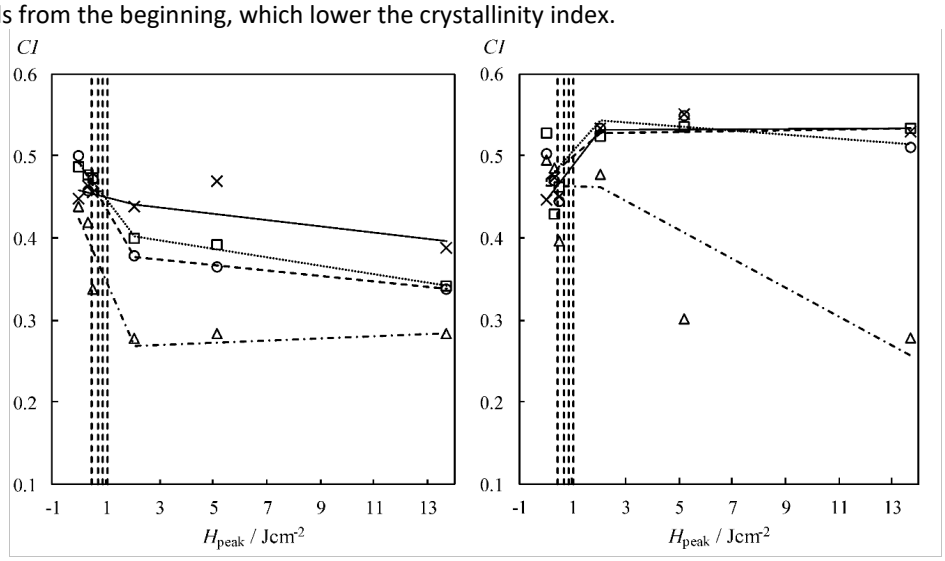


Fig. 5. Crystallinity index of the irradiated (left) as well as irradiated and aqueous extracted substrates (right) as a function of the laser fluence. Linters: solit lines, crosses; sulfate: dotted lines, squares; sulfite: dashed lines, circles; CTMP: dotted-dashed lines, triangles. Lines are first-degree polynomial regressions by section and illustrate the principle progression. Vertical lines between 0 $Jcm^{-2}$ and 2 $Jcm^{-2}$ are the threshold fluences of the ablation regime of the respective substrate (compare Table 2).

### *3.4. Transfer to joining process*

The transfer of the knowledge gained into areas of industrial relevance is aimed at through the realization of joints without filler material. The laser parameters of the local irradiation were selected according to empirical aspects to increase the proportion of melt-like reaction products. A heat sealing machine (HSG/ETK, Brugger) then enables the joining of 5 mm wide stripes with a sealing pressure of 36 bar and a temperature of 200 °C. After an acclimatization at 23 °C and 50 % relative humidity, the adhesion of the seal samples is tested with a tensile testing maschine (TT 2805, Tira) in the T-Peel test.

The CTMP substrate exhibits the highest tensile strength, due to the high lignin content, which already shows a reduction in viscosity at low temperatures. Likewise, high strengths can be achieved with the sulfate substrate. The reason for this is high hemicellulose content, which ensures an increased proportion of resolidified reaction products. Linters and sulfite have a lower hemicellulose and lignin content and exhibit lower bond strengths. To demonstrate what is immediately technically possible, two additional substrates coated with additives were irradiated and sealed. The bond strengths of the more complex papers are in the so-called "easy-peel" range. This is used for the design of joints that are to be released with little force.

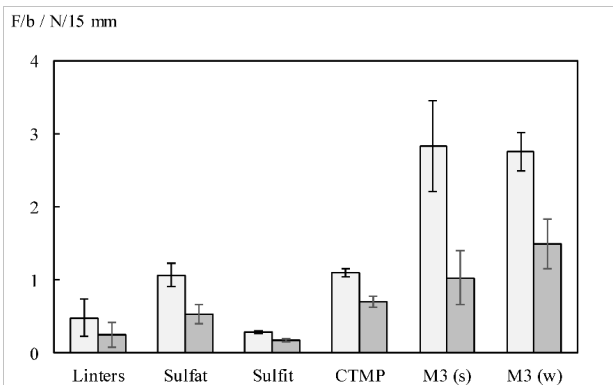


Fig. 6. Maximum (light grey) and average (dark grey) width related breaking strength of the four original paper substrates and, as an example, of two paper substrates provided with additives (starch and wet strength agent).

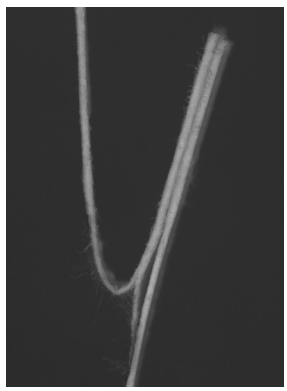

Fig. 7. Side view of joined papers in the T-Peel test. Failure of the connection in the paper, next to the joint.

## 4. Summary

The aim of the investigations was to gain fundamental knowledge about the interaction of CO laser radiation and classic paper materials and to develop this further in the direction of a joining process. Four papers with different proportions of the basic paper components cellulose, hemicellulose and lignin were intensively investigated by microscopy, IR spectroscopy and high-speed videography. During irradiation, a liquid state could be observed, which was identified as an intermediate step of the highly dynamic pyrolytic decomposition. By IR spectroscopy, short-chain saccharides are confirmed as resolidified reaction products. These exhibit a melt-like reduction in viscosity due to the lower degree of polymerization in a temperature range around 200 °C. Irradiation of the papers followed by a heat sealing process thus allows joining without the need for filler materials foreign to the material. The bond strength of the joint was finally verified in a T-peel test.

## 5. Literature

Back, E. L. ; Nordin, S. B. ; Nyrén, J.: An Indication of Molten Cellulose Produced in a Laser Beam - additional informations. In: Textile Research Journal (1974)

Back, E. L.: Cellulose bei hohen Temperaturen: Selbstvernetzung, Glasumwandlung und Schmelzen unter Einwirkung von Laserstrahlen. In: Papier 27 (1973), S. 475–483

Bansa, H. (Hrsg.); Brannahl, G. (Hrsg.); Köttelwesch, C. (Hrsg.); Wächter, O. (Hrsg.): Dauerhaftigkeit von Papier, 1979

Boutin, O. ; Ferrer, M. ; Lédé, J.: Radiant flash pyrolysis of cellulose—Evidence for the formation of short life time intermediate liquid species. In: Journal of Analytical and Applied Pyrolysis 47 (1998), S. 13–31

Boutin, O. ; Ferrer, M. ; Lédé, J.: Flash pyrolysis ofcellulose pellets submitted to a concentrated radiation: experiments and modelling. In: Chemical Engineering Science 57 (2002), S. 15–25

Delagoutte, T.: Contaminants Impact and Management in Recycled Pulps. In: centre technique du papier (Hrsg.): Avanced training course on “deinking and recycling”, 2015

Hamann, L.: Stickies: Definition, Origin and Characterization. In: centre technique du papier (Hrsg.): Avanced training course on “deinking and recycling”, 2015

Hurtubise, F. G. ; Krassig, H.: Classification of Fine Structural Characteristics in Cellulose by Infared Spectroscopy. In: Analytical Chemistry 32 (1960), Nr. 2, S. 177–181

Kolar, J. ; Strlic, M. ; Pentzien, S. ; Kautek, W.: Near-UV, visible and IR pulsed laser light interaction with cellulose. In: Applied Physics A 71 (2000), S. 87–90

Liu, J. M.: Simple technique for measurements of pulsed Gaussian-beam spot sizes. In: Optics Letters 7 (1982), S. 196–198 – Überprüfungsdatum 2019-10-15

Nelson, M. L. ; O´Connor, R. T.: Relation of certain infrared bands to cellulose crystallinity and crystal lattice type. Part II. A new infrared ratio for estimation of crystallinity in celluloses I and II. In: Journal of Applied Polymer Science 8 (1964), S. 1325–1341 – Überprüfungsdatum 2019-06-12

Nelson, M. L. ; O´Connor, R. T.: Relation of certain infrared bands to cellulose crystallinity and crystal latticed type. Part I. Spectra of lattice types I, II, III and of amorphous cellulose. In: Journal of Applied Polymer Science 8 (1964), S. 1311–1324

Nordin, S. B. ; Nyren, J. O. ; Back, E. L.: An Indication of Molten Cellulose Produced in a Laser Beam. In: Textile Research Journal (1974)

O'Sullivan, A. C.: Cellulose: the structure slowly unravels. In: Cellulose 4 (1997), S. 173–207

Segal, L. ; Creely, J. J. ; Martin, A. E. ; Conrad, C. M.: An empirical method for estimating the degree of crystallinity of native cellulose using the X-Ray diffractometer. In: Textile Research Journal 29 (1959), S. 786–794

Shafizadeh, F. ; Furneaux, R. H. ; Cochran, T. G. ; Scholl, J. P. ; Sakai, Y.: Production of levoglucosan and glucose from pyrolysis of cellulosic materials. In: Journal of Applied Polymer Science 23 (1979), S. 3525–3539

Shimazu, F. ; Sterling, C.: Effect of Wet and Dry Heat on Structure of Cellulose. In: Journal of Food Science 31 (1966), S. 548–551

Suzuki, J. ; Azuma, J.-I. ; Koshijima, T. ; Okamura, K. ; Okamoto, H.: Characterization of mono- and oligosaccarides produced by CO2 laser irradiation an cellulose. In: Chemistry Letters (1983), S. 481–484

Yang, H. ; Yan, R. ; Chen, H. ; Lee, D. H. ; Zheng, C.: Characteristics of hemicellulose, cellulose and lignin pyrolysis. In: Fuel 86 (2007), 12-13, S. 1781–1788

Yeo, J. Y. ; Chin, B. L. F. ; Tan, J. K. ; Loh, Y. S.: Comparative studies on the pyrolysis of cellulose, hemicellulose, and lignin based on combined kinetics. In: Journal of the Energy Institute 92 (2019), Nr. 1, S. 27–37